International Journal of Biochemistry and Cell Biology 113 (2019) 58–66

Contents lists available at ScienceDirect

International Journal of Biochemistry and Cell Biology

journal homepage: www.elsevier.com/locate/biocel

Inhibition of dendritic spine extension through acrolein conjugation with α-, β-tubulin proteins

Takeshi Uemura[a,b], Takehiro Suzuki[c], Kenta Ko[b], Kenta Watanabe[b], Naoshi Dohmae[c], Akihiko Sakamoto[d], Yusuke Terui[d], Toshihiko Toida[b], Keiko Kashiwagi[d], Kazuei Igarashi[a,b,*]

[a] Amine Pharma Research Institute, Innovation Plaza at Chiba University, 1-8-15 Inohana, Chuo-ku, Chiba, Chiba, 260-0856, Japan
[b] Graduate School of Pharmaceutical Sciences, Chiba University, 1-8-1 Inohana, Chuo-ku, Chiba, Chiba, 260-8675, Japan
[c] RIKEN Center for Sustainable Resource Science, 2-1 Hirosawa, Wako, Saitama, 351-0198, Japan
[d] Faculty of Pharmacy, Chiba Institute of Science, 15-8 Shiomi-cho, Choshi, Chiba, 288-0025, Japan

ARTICLE INFO

Keywords:
Acrolein
Brain infarction
α-, β-tubulins
Cysteine
Microtubule
Dendritic spine

ABSTRACT

We have recently found that conjugation of acrolein with a 50 kDa protein(s) is strongly associated with tissue damage during brain infarction. In the current study, the identity and function of the 50 kDa protein(s) conjugated with acrolein during brain infarction were investigated. The 50 kDa protein(s) conjugated with acrolein were identified as α- and β-tubulins. Ten cysteine residues in α- and β-tubulins (Cys25, 295, 347 and 376 in α-tubulin and Cys12, 129, 211, 239, 303 and 354 in β-tubulin) were mainly conjugated with acrolein. Since two cysteine residues of α-tubulin (Cys347 and 376) and four cysteine residues of β-tubulin (Cys12, 129, 239 and 354) were located at the interaction site of α- and β-tubulins, association between α- and β-tubulins to form microtubules was strongly inhibited by conjugation with acrolein. Accordingly, dendritic spine extension consisting of microtubules was greatly inhibited in acrolein-treated Neuro2a cells. The results strongly suggest that acrolein contributes to the functional losses in brain signaling through its conjugation with α- and β-tubulins.

1. Introduction

It is thought that cell damage is mainly caused by reactive oxygen species (ROS) consisting of superoxide anion ($O_2^{\cdot -}$), hydrogen peroxide (H_2O_2), and hydroxyl radical ($^{\cdot}OH$) (Giorgio et al., 2007). However, we found that acrolein ($CH_2=CH-CHO$) produced mainly from spermine [$NH_2(CH_2)_3NH(CH_2)_4NH(CH_2)_3NH_2$], one of the polyamines, essential for cell growth and viability (Igarashi and Kashiwagi, 2019; Pegg, 2009), is more toxic than ROS using a cell culture system (Igarashi et al., 2018; Sharmin et al., 2001; Yoshida et al., 2009). Acrolein is spontaneously formed from 3-aminopropanal [$NH_2(CH_2)_2CHO$] produced from spermine by spermine oxidase. Acrolein is also produced less effectively from oxidation of spermine by spermidine/spermine N^1-acetyltransferase and acetylpolyamine oxidase (Kimes and Morris, 1971; Wang and Casero, 2006). Although acrolein was first thought to be produced from unsaturated fatty acids (Uchida et al., 1998b), acrolein production from unsaturated fatty acids is minimal (Bradley et al., 2010; Tomitori et al., 2005).

Then, we found that the size of stroke was nearly parallel with the multiplied value of protein-conjugated acrolein (PC-Acro) and total polyamine oxidases (spermine oxidase plus acetylpolyamine oxidase) in plasma (Tomitori et al., 2005). We also found that measurement of PC-Acro together with interleukin-6 and C-reactive protein in plasma makes it possible to identify a small infarction, i. e. silent brain infarction, with high sensitivity (84%) and specificity (84%) (Yoshida et al., 2010). In addition, acrolein scavengers such as *N*-acetylcysteine (NAC) (Saiki et al., 2009) and its derivatives (Saiki et al., 2011; Uemura et al., 2018) decreased the size of brain infarction and had protective effects against brain infarction (Uemura et al., 2018) in photochemcally induced thrombosis (PIT) mice. In humans, early identification of a small infarction may help sustain a better quality of life in elderly patients through suitable treatment.

With regard to acrolein toxicity, we found that acrolein-conjugated glyceraldehyde-3-phosphate dehydrogenase (GAPDH) translocated to the nucleus and caused apoptosis in mouse mammary carcinoma FM3A cells and neuroblastoma Neuro2a cells (Nakamura et al., 2013), and that acrolein stimulated matrix metalloproteinase (MMP)-9 activity leading to tissue damage (Uemura et al., 2017a). In this study, we

Abbreviations: LC–MS/MS, liquid chromatography–tandem mass spectrometry; NAC, *N*-acetylcysteine; PC-Acro, protein-conjugated acrolein; PIT, photochemically induced thrombosis

* Corresponding author at: Amine Pharma Research Institute, Innovation Plaza at Chiba University, 1-8-15 Inohana, Chuo-ku, Chiba, Chiba, 260-0856, Japan.
E-mail address: iga16077@faculty.chiba-u.jp (K. Igarashi).

https://doi.org/10.1016/j.biocel.2019.05.016
Received 9 March 2019; Received in revised form 24 May 2019; Accepted 27 May 2019
Available online 28 May 2019
1357-2725/

sought to identify acrolein-conjugated protein(s) generated after a stroke using an *in vivo* mouse model and neuroblastoma Neuro2a cells. It was found that the major acrolein-conjugated proteins were α-, β-tubulin proteins. The effects of acrolein on formation of cytoskeleton were also examined.

2. Materials and methods

2.1. Induction of brain stroke in mice

All animal experiments were approved by the Institutional Animal Care and Use Committee of Chiba University and performed according to the Guidelines for Animal Research of Chiba University. Induction of brain stroke was conducted by photochemically induced thrombosis (PIT) technique using 12-month-old male C57BL/6 mice (22–26 g) as described previously (Saiki et al., 2013, 2009). Mice were anesthetized with inhalation of 3% isoflurane (Abbot Japan), and then maintained with 1.5% isoflurane during operation using a small-animal anesthesia system. For induction of ischemia, immediately after intravenous injection of photosensitizer Rose Bengal (20 mg/ kg) through a jugular vein, green light (wave length, 540 nm) emitted from a xenon lamp (Hamamatsu Photonics, Japan) illuminated the middle cerebral artery for 10 min. At 24 h after the induction of PIT stroke, the brains were removed and stored for further use. If necessary, the locus of brain infarction was confirmed by staining with a triphenyltetrazolium chloride solution (Saiki et al., 2009).

2.2. Measurement of PC-Acro

Approximately 2 mg of mouse brain tissues from both control and stroke mice were homogenized using 1.5 mL with a disposable Power Masher II homogenizer (Nippi, Japan) in 100 μL of buffer A containing 50 mM Tris − HCl, pH 7.6, 150 mM NaCl, 1% Nonidet P-40, 0.5% sodium deoxycholate, 0.1% SDS, 10 μg/mL aprotinin, 500 μM sodium orthovanidate and 10 μg/mL phenylmethylsulfonyl fluoride. Thirty μg of protein was separated on a 10% SDS-polyacrylamide gel and transferred electrophoretically to a PVDF membrane (Merck Millipore). Blots were blocked in 1% bovine serum albumin in Tris-buffered saline containing 0.1% Tween 20 (TBS-T) for 30 min at room temperature. Protein-conjugated acrolein (PC-Acro, [N^{ε}-(3-formyl-3,4-dehydropiperidino)lysine (FDP-lysine), and N^{ε}-(3-methylpyridinium)lysine (MP-lysine) in protein]) was detected by an ECL (electrochemiluminescence) Western Blotting Detection System (GE Healthcare) using anti-PC-Acro (NOF Corp., Japan) as a primary antibody with 1/2000 dilution. The level of β-actin was detected using anti-β-actin antibody (Santa Cruz Biotechnology) as a primary antibody with 1/10000 dilution. The amount of protein was determined by BCA (bicinchoninic acid) protein assay kit (Nacalai Tesque) using bovine serum albumin as a standard (Smith et al., 1985).

2.3. Identification of acrolein modified 50 kDa proteins as α- and β-tubulins and of acrolein conjugated amino acid residues in tubulins

Identification of 50 kDa proteins was performed as reported (Uemura et al., 2017a). A 50 kDa protein band in which acrolein conjugation was increased during infarction was excised and digested in gel with trypsin (TPCK-treated, Worthington Biochem. Co.) at 37 °C overnight. The band was identified as α- and β-tubulin proteins using LC−MS/MS.

For identification of acrolein-conjugated amino acid residues in α- and β-tubulins, purified porcine brain tubulin proteins were purchased from Cytoskeleton, Inc. A hundred ng of tubulin proteins were incubated with 10 μM of acrolein in 50 μL of buffer B containing 80 mM PIPES, pH 6.9, 2 mM $MgCl_2$, 0.5 mM EGTA and 1 mM GTP at 37 °C for 2 h. After incubation, proteins were subjected to the SDS-PAGE. The 50 kDa protein band was excised, reduced with dithiothreitol and alkylated by acrylamide. The protein in-gel was digested with either trypsin or endoproteinase Asp-N (Roche Applied Science) at 37 °C overnight. An aliquot of digestion mixture was separated using a nano-electrospray ionization spray column (NTCC analytical column, C18, φ75 μm × 100 mm, 3 μm; Nikkyo Technos, Tokyo, Japan) with a linear gradient of 0–64% buffer C (100% acetonitrile and 0.1% formic acid) at a flow rate of 300 nL/min over 30 min, and subjected on-line to a Q-Exactive mass spectrometer (Thermo Fisher Scientific, Inc.) that was equipped with a nanospray ion source. MS (resolution 70,000) and MS/MS (resolution 17,500) data were acquired in a data-dependent TOP10 method. Obtained MS and MS/MS data were quantified with Proteome Discoverer 2.2 (Thermo Scientifc) using MASCOT search engine Version 2.3 (Matrix Science) against the Swiss-Prot 2015-08 or in-house database (containing tubulins, P02554, P02550, Q2XVP4, Q767L7) using the following parameters: taxonomy, Mammals (66,386 sequences); type of search, MS/MS ion search; enzyme, trypsin and/or Asp-*N*-ambic; fixed modification, none; variable modifications, Gln- > N pyro-Glu (N-term Q), oxidation (M), propionamide (C), deamidated (NQ), acrolein adduct (C), acrolein adduct 2 (N-term), MP-lysine (K), FDP-lysine (K), and Nim-propanalhistidine (H); mass values, monoisotopic; peptide mass tolerance, 20 ppm; fragment mass tolerance, ± 0.05 Da; peptide charge, 1 +, 2 + and 3 +; instrument type, ESI-TRAP. An acrolein conjugated with cysteine is shifted at the N-terminus of the peptide by Michael addition and a Schiff base is formed (Bradley et al., 2010).

2.4. Determination of the level of normal and acrolein-conjugated tubulins in brain

The level of normal and acrolein-conjugated tubulins was analyzed by immunoprecipitation using the method described previously (Uemura et al., 2008). One hundred μg protein of brain tissue lysate was incubated with 1 μL of anti-β-tubulin antibody (Proteintech) in 50 μL of buffer D containing 50 mM Tris − HCl, pH 8.0, 1 mM EDTA, 120 mM NaCl and 0.5% NP-40 at 4 °C for 16 h, and the antibody was collected with 10 μL of the Protein A Mag Sepharose™ beads (GE Healthcare) with an additional 16 h incubation with gentle rotation. Beads were suspended in 40 μL of SDS-sample loading buffer and boiled for 5 min. Proteins were separated on a 10% SDS-polyacrylamide gel, and total and acrolein-conjugated tubulin proteins were detected as described above.

2.5. Tubulin polymerization assay

The effect of acrolein on polymerization of tubulin proteins was analyzed using the tubulin polymerization assay kit with purified tubulin proteins (Cytoskeleton, Inc.) according to the manufacturer's protocol in a 96-plate format. The assay was carried out at 37 °C in the presence or absence of 10 μM acrolein and/or 15% glycerol in 100 μL of reaction mixture consisted of 2 mg/mL tubulin proteins, 80 mM PIPES, pH 6.9, 1 mM GTP, 2 mM $MgCl_2$ and 0.5 mM EGTA. The fluorescence intensity was measured every 5 min using a microplate reader SH-9000 (Corona Electric, Japan).

2.6. Determination of α-tubulin associated with β-tubulin

A hundred ng of purified tubulin proteins (Cytoskeleton, Inc.) were incubated with 10 μM of acrolein in 50 μL of buffer B containing 80 mM PIPES, pH 6.9, 2 mM $MgCl_2$, 0.5 mM EGTA in the presence or absence of 1 mM GTP at 37 °C for 2 h. The α- and β-tubulin complex was pulled down using anti-β-tubulin antibody (Sigma) as described above and α-tubulin protein associated with β-tubulin was detected by Western blotting using an anti-α-tubulin antibody (Proteintech). Relative amounts of proteins were measured using the ImageJ program (NIH, https://imagej.nih.gov/ij/) from three independent experiments and plotted as mean + SD in bar graphs.

2.7. Indirect immunofluorescence microscopy

Mouse neuroblastoma Neuro2a cells (DS Pharma Biomedical Co., Ltd.) were inoculated on cover slips in 2 mL of DMEM (Nacalai Tesque) supplemented with 50 U/mL streptomycin, 100 U/mL penicillin G and 10% fetal bovine serum at the density of 10^3 cells/cm^2 and cultured at 37 °C in an atmosphere of 5% CO_2, with or without 10 μM acrolein for 24 h. Cells were washed three times with phosphate buffered saline (PBS) and fixed in 2% paraformaldehyde at 37 °C for 15 min, then soaked in acetone at −20 °C for 15 s. Staining β-tubulin in cells was carried out as previously reported (Uemura et al., 2017b). In brief, coverslips with cells were treated with 1% bovine serum albumin in PBS and incubated with 1,000-fold diluted anti-β-tubulin (Proteintech) at 4 °C for 16 h, washed 10 times with PBS and incubated with Alexa Fluor 486 labeled secondary antibody (Invitrogen) at 4 °C for 16 h. After washing 10 times with PBS, cells were mounted in Prolong Gold Mounting Solution (Clontech). Fluorescence signals of β-tubulin were visualized using an Evos FL Auto 2 fluorescence microscope with Celleste image analysis software (Invitrogen).

2.8. Immunofluorescence staining of brain tissue

Brain tissue was taken out at 24 h after induction of ischemia and fixed in 4% paraformaldehyde at 4 °C for 16 h and paraffin embedded. A 4 μm thin section was cut and mounted on a slide glass. Tissue was deparaffinized with xylene and antigen was retrieved with Histo VT one solution (Nacalai Tesque) according to the manufacturer's protocol. Tubulin was stained with anti-β-tubulin antibody (Proteintech, 1/500 dilution) as a primary antibody and Alexa fluor 488 conjugated anti-Rabbit IgG (Invitrogen, 1/1000 dilution) as a secondary antibody. The slice was mounted with Prolong Gold Mounting Solution (Clontech). Fluorescence signals of β-tubulin were visualized using an Evos FL Auto 2 fluorescence microscope with Celleste image analysis software (Invitrogen).

2.9. Statistical analysis

Statistical analysis was performed using GraphPad Prism version 8.1 for Mac, GraphPad Software, La Jolla California USA, www.graphpad.com. Differences between two groups were compared using Student's t-test. For comparison of multiple groups, one-way ANOVA followed by Dunnett's multiple comparisons test was used. A p-value < 0.05 was considered statistically significant.

3. Results

3.1. Identification of α- and β-tubulins as major acrolein-conjugated proteins during brain stroke

To identify which proteins are conjugated with acrolein following a stroke, proteins in brain tissue from three control and stroke mice were separated by gel electrophoresis, and the levels of PC-Acro were analyzed by Western blotting (Fig. 1A). In the stroke model, compared to controls, levels of approximately 65 kDa proteins [mainly albumin exuded from blood (Saiki et al., 2009)] increased, but there was a decrease in proteins with high molecular mass more than 200 kDa, suggesting that higher molecular mass proteins may be degraded by proteases during stroke (Fig. 1a, CBB staining). We have reported previously that the activity of MMP-9, an extracellular protease, is stimulated by acrolein (Uemura et al., 2017a). However, an increase in acrolein-conjugated proteins was clearly observed at 50 kDa protein(s) (Fig. 1A, PC-Acro), suggesting that these 50 kDa protein(s) are associated with tissue damage during stroke. Thus, identification of these 50 kDa protein(s) was carried out through determination of amino acid sequences by LC–MS/MS analysis. The identified sequences are shown in red (Fig. 1B), and were parts of peptides that comprise α- and β-tubulins. Under these conditions, the level of β-actin (42 kDa) was nearly equal in normal and infarct brain (Fig. 1A).

The residues that are conjugated with acrolein within α- and β-tubulins were determined using purified α- and β-tubulins. As shown in Fig. 2A, ten cysteine residues were conjugated with acrolein. Those were Cys25, 295, 347 and 276 in α-tubulin and Cys12, 129, 211, 239, 303 and 354 in β-tubulin. Mass spectra of the peptides 345–365 of α-tubulin and the peptides 3–19 of β-tubulin were shown in Fig. 3. The results indicate that Cys347 of α-tubulin and Cys12 of β-tubulin were conjugated with acrolein. These acrolein-conjugated ten cysteine residues were indicated in red on a three-dimentional structure of α- and β-tubulins (Fig. 2B) (Alushin et al., 2014). Two cysteine residues of α-tubulin (Cys347 and 376) and four residues of β-tubulin (Cys12, 129, 239 and 354) were located at the interaction site of α- and β-tubulins, suggesting that interaction between α- and β-tubulins may be disturbed by acrolein conjugation. The level of PC-Acro was estimated using an antibody recognizing acrolein-conjugated lysines, *i.e.* FDP-lysine [N^{ε}-(3-formyl-3,4-dehydropiperidino)lysine] and MP-lysine [N^{ε}-(3-methylpyridinium)lysine] (Uchida et al., 1998a). However, the levels of FDP- and MP-lysines in α- and β-tubulins were very low compared with those of acrolein-conjugated cysteines (Fig. 2).

To verify that β-tubulin is an acrolein-conjugated protein at the locus of the ischemic stroke, β-tubulin was immunoprecipitated from brain homogenate of control and stroke mice. Immunoprecipitated proteins were separated by SDS-PAGE and analyzed by Western blotting using anti-β-tubulin (Fig. 4A) and anti-PC-Acro (Fig. 4B). The protein levels of β-tubulin were nearly equal between normal and ischemic brain (Fig. 4A), but the conversion to the acrolein conjugated β-tubulin was mainly observed at the locus of ischemia compared to controls (Fig. 4B).

3.2. Decrease in the polymerization of α- and β-tubulins through acrolein conjugation

It is known that microtubule polymerization of α- and β-tubulins is dependent on GTP, and is enhanced by high concentrations of glycerol (Keates, 1980). Thus, effects of acrolein on the polymerization of α- and β-tubulins was examined in the presence and absence of 15% glycerol. As shown in Fig. 5, the degree of polymerization was slightly inhibited by 10 μM acrolein in the presence of glycerol (Fig. 5A), whereas it was greatly inhibited by 10 μM acrolein in the absence of glycerol (Fig. 5B).

To further confirm that acrolein inhibits association of α- and β-tubulins, tubulin proteins were incubated in the presence and absence of 1 mM GTP and 10 μM acrolein at 37 °C for 2 h. The association was estimated by immunoprecipitation with anti-β-tubulin antibody (Fig. 6). The association between α- and β-tubulins was inhibited approximately 70% by acrolein (Fig. 6A), but the recovery of β-tubulin by immunoprecipitation was inhibited only 10% by acrolein (Fig. 6B). GTP did not influence the association between two tubulins.

To confirm the acrolein inhibition of association of α- and β-tubulins, dendritic spine extension of Neuro2a cells was estimated by the indirect immunofluorescence microscopy. Cells were cultured with or without 10 μM acrolein for 24 h. As shown in Fig. 7A, dendritic spine extension, shown in green fluorescence, was greatly inhibited through acrolein conjugation with α- and β-tubulins. Dendritic spine extension of Neuro2a cells was almost negligible in the presence of acrolein. Inhibition of dendritic spine formation was also confirmed in brain tissue (Fig. 7B). The size of dendritic spine shown in green fluorescence of β-tubulins at the locus of brain infarction was significantly smaller than that of dendritic spine in the normal brain. These results indicate that acrolein inhibits dendritic spine extension through the inhibition of microtubule formation consisting of α- and β-tubulins during brain infarction.

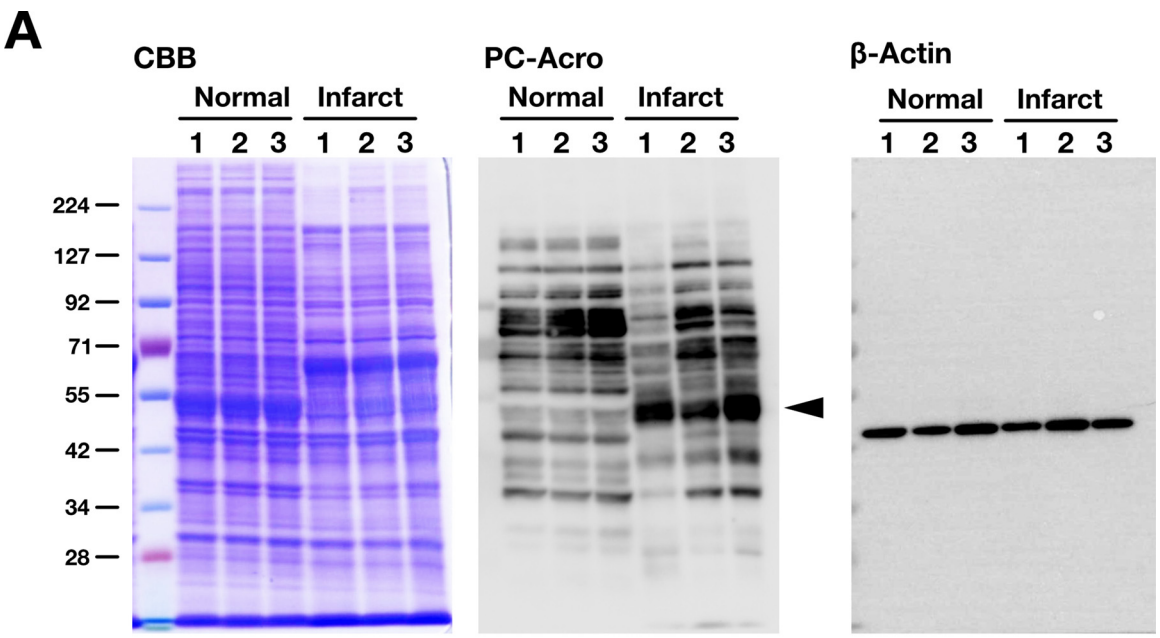

B

α-Tubulin

```
  1  MRECISIHVG QAGVQIGNAC WELYCLEHGI QPDGQMPSDK TIGGGDDSFN TFFSETGAGK
 61  HVPRAVFVDL EPTVIDEVRT GTYRQLFHPE QLITGKEDAA NNYARGHYTI GKEIIDLVLD
121  RIRKLADQCT GLQGFLVFHS FGGGTGSGFT SLLMERLSVD YGKKSKLEFS IYPAPQVSTA
181  VVEPYNSILT THTTLEHSDC AFMVDNEAIY DICRRNLDIE RPTYTNLNRL ISQIVSSITA
241  SLRFDGALNV DLTEFQTNLV PYPRIHFPLA TYAPVISAEK AYHEQLSVAE ITNACFEPAN
301  QMVKCDPRHG KYMACCLLYR GDVVPKDVNA AIATIKTKRS IQFVDWCPTG FKVGINYQPP
361  TVVPGGDLAK VQRAVCMLSN TTAIAEAWAR LDHKFDLMYA KRAFVHWYVG EGMEEGEFSE
421  AREDMAALEK DYEEVGVDSV EGEGEEEGEE Y
```

β-Tubulin

```
  1  MREIVHIQAG QCGNQIGAKF WEVISDEHGI DPTGTYHGDS DLQLDRISVY YNEATGGKYV
 61  PRAILVDLEP GTMDSVRSGP FGQIFRPDNF VFGQSGAGNN WAKGHYTEGA ELVDSVLDVV
121  RKEAESCDCL QGFQLTHSLG GGTGSGMGTL LISKIREEYP DRIMNTFSVV PSPKVSDTVV
181  EPYNATLSVH QLVENTDETY CIDNEALYDI CFRTLKLTTP TYGDLNHLVS ATMSGVTTCL
241  RFPGQLNADL RKLAVNMVPF PRLHFFMPGF APLTSRGSQQ YRALTVPELT QQVFDAKNMM
301  AACDPRHGRY LTVAAVFRGR MSMKEVDEQM LNVQNKNSSY FVEWIPNNVK TAVCDIPPRG
361  LKMAVTFIGN STAIQELFKR ISEQFTAMFR RKAFLHWYTG EGMDEMEFTE AESNMNDLVS
421  EYQQYQDATA EEEEDFGEEA EEEA
```

Fig. 1. Identification of acrolein-conjugated proteins as α- and β-tubulins following a stoke. A. SDS-PAGE was performed using 30 μg proteins obtained from control and ischemic brain from 3 individual mice, and Western blotting was performed using antibody recognizing acrolein-conjugated lysine. The level of β-actin is shown as a loading control. CBB, Coomassie brilliant blue staining. B. Amino acid sequences of 50 kDa proteins (indicated by an arrow in Fig. 1A) were determined by LC–MS/MS. Identified peptide sequences in α- and β-tubulins by LC–MS/MS are shown in red.

A. Identified peptide sequences with acrolein addition

Position	Peptide sequence	Acrolein modification	Observed Mr (Charge)	Calculated Mr (Charge)
α-tubulin				
22 - 32	ELY**C**LEHGIQP	N-terminal	670.3207 (2+)	670.3212 (2+)
290 - 296	EITNA**C**F	N-terminal	418.1866 (2+)	418.1864 (2+)
345 - 366	DW**C**PTGFKVGINYQPPTVVPGG	N-terminal	1185.5775 (2+)	1185.5830 (2+)
367 - 385	DLAKVQRAV**C**MLSNTTAIA	N-terminal	681.6947 (3+)	681.6957 (3+)
β-tubulin				
3 - 19	EIVHIQAGQ**C**GNQIGAK	N-terminal	601.9785 (3+)	601.9772 (3+)
128 - 156	D**C**LQGFQLTHSLGGGTGSGMGTLLISKIR	N-terminal	995.8450 (3+)	995.8477 (3+)
209 - 223	DI**C**FRTLKLTTPTYG	N-terminal	589.6441 (3+)	589.6430 (3+)
224 - 248	DLNHLVSATMSGVTT**C**LRFPGQLNA	N-terminal	895.1151 (3+)	895.1159 (3+)
295 - 303	DAKNMMAA**C**	N-terminal	992.3943 (1+)	992.3998 (1+)
327 - 354	DEQMLNVQNKNSSYFVEWIPNNVKTAV**C**	N-terminal	1103.5228 (3+)	1103.5287 (3+)

B. Acrolein modified cysteine residues on tubulin proteins

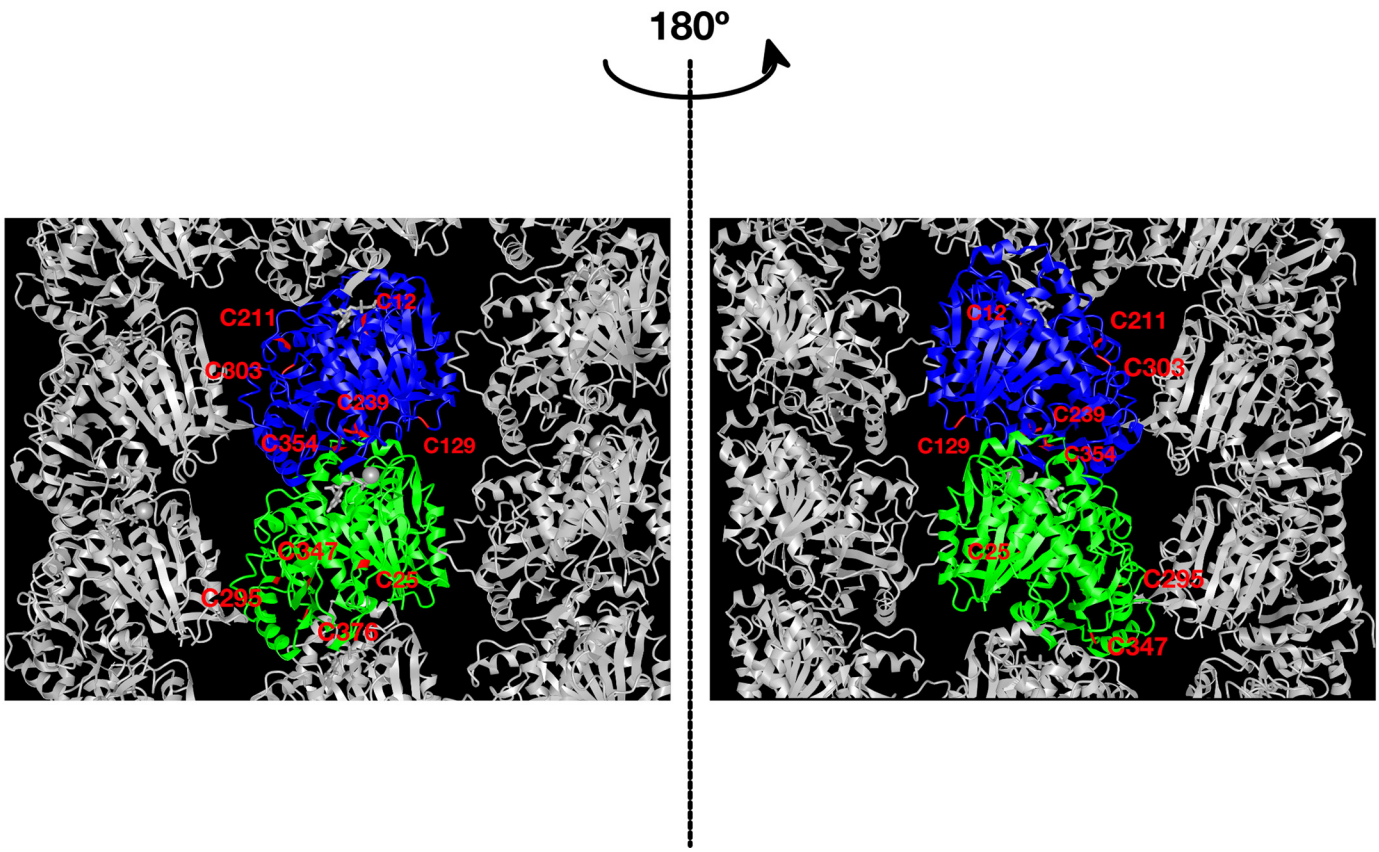

Fig. 2. Identification of acrolein-conjugated amino acid residues in α- and β-tubulins. A. Peptide sequences containing acrolein-conjugated amino acids determined by LC–MS/MS. Cysteine residues shown in red were acrolein-conjugated cysteines. B. Location of acrolein-conjugated cysteine residues on the α- and β-tubulin complex (Alushin et al., 2014). Green, α-tubulin; blue, β- tubulin.

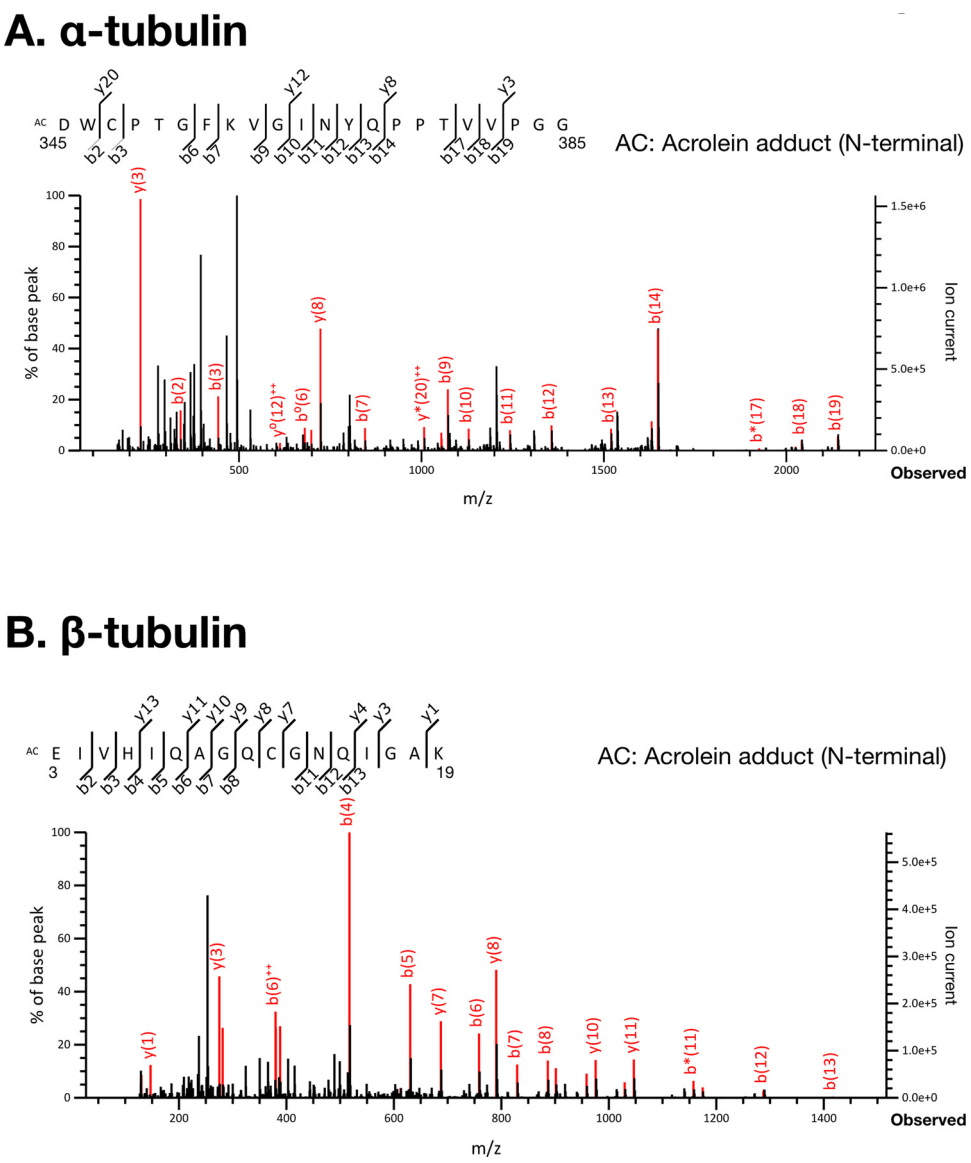

Fig. 3. Identification of acrolein-conjugated amino acid residues in α- and β-tubulins. MS/MS spectra of the peptide 345–366 of α-tubulin (A) and the peptide 3–19 of β-tubulin (B) containing cysteine residues conjugated with acrolein were shown. Cys347 of α-tubulin and Cys12 of β-tubulin were conjugated with acrolein by Michael addition, and Schiff base was formed intramolecularly at the N-terminus of the peptide as described in Materials and methods.

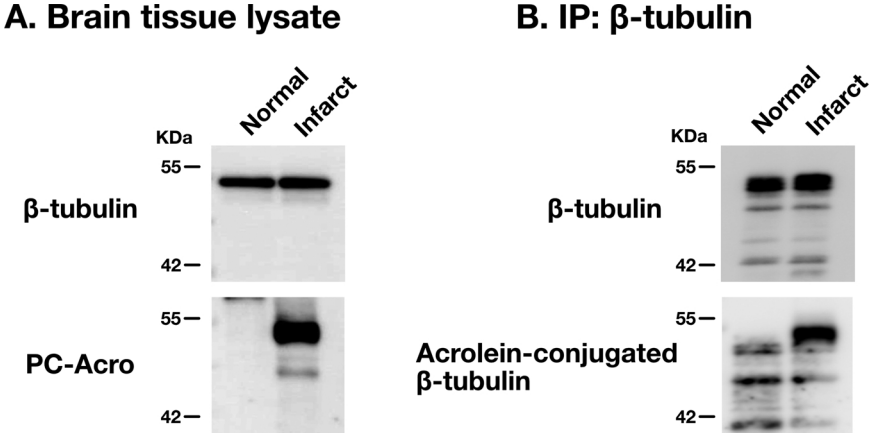

Fig. 4. Increase in acrolein-conjugated β-tubulin during infarction. The levels of β-tubulin and acrolein-conjugated proteins in 100 μg protein of brain tissue lysate from normal and ischemic brain were measured by SDS-PAGE and Western blotting (A). The level of acrolein-conjugated β-tubulin in normal and ischemic brain were measured by SDS-PAGE and Western blotting after immunoprecipitation with 1 μL of anti-β-tubulin antibody (Proteintech) (B). The results were repeatable in three experiments.

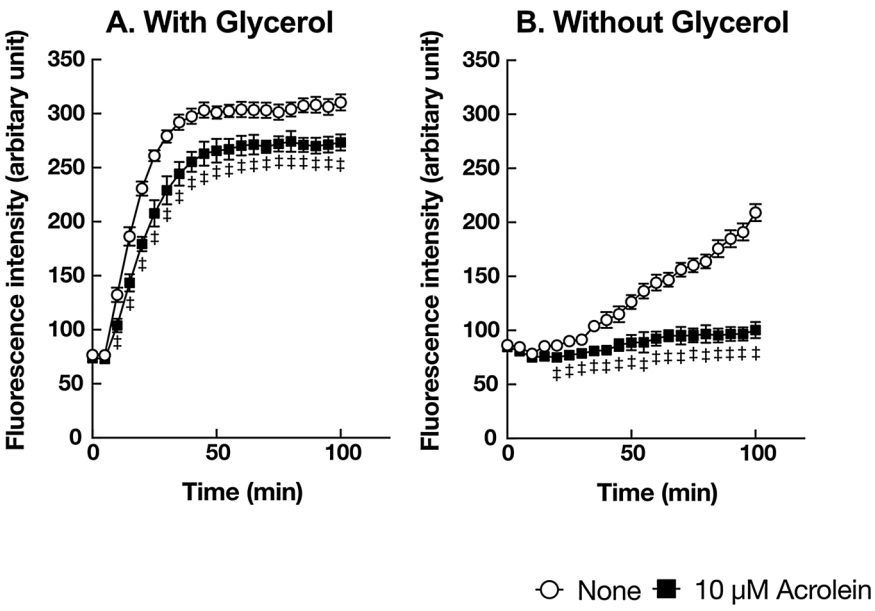

Fig. 5. Acrolein inhibition of polymerization of α- and β-tubulins. Effect of 10 μM acrolein on the polymerization of α- and β-tubulins was examined in the presence (A) and absence (B) of 15% glycerol as described in Materials and methods. Data are shown as mean ± S. D. of three experiments. ○, none; ■, 10 μM acrolein. ‡, $p < 0.05$.

4. Discussion

It has been reported that the microtubules are important for some aspects of normal brain function (Janke and Bulinski, 2011; Pchitskaya et al., 2018). In this study, it was found that α- and β-tubulins, which are components of microtubules, were damaged by acrolein following brain ischemia. Inhibition of tubulin polymerization by acrolein was higher in the absence of glycerol rather than in the presence of glycerol. As glycerol stabilizes the microtubule structure (Keates, 1980), the results suggest that acrolein conjugation inhibits incorporation of tubulin proteins into microtubules rather than dissociation of the existing microtubules. This idea was confirmed with the results showing acrolein inhibited dimer formation of α- and β-tubulins which is essential for the microtubule polymerization (Fig. 6). Acrolein conjugation at cysteine residues on the contact surface (Cys347 and 376 of α-tubulin and Cys12, 129, 239 and 354 of β-tubulin) probably contributes to the inhibition of tubulin polymerization. It is also noted that GTP has small effect on the inhibition of dimer formation by acrolein. Dendritic spine extension was strongly inhibited by acrolein in Neuro2a cells, likely as a consequence of the inhibition of microtubule formation. It was also reported that actin, a component of microfilament, was conjugated with acrolein at Cys374 (Dalle-Donne et al., 2007). Furthermore, we found that vimentin, a component of intermediate filaments, is conjugated with acrolein (unpublished results). These results indicate that the cytoskeleton is strongly damaged by acrolein, because three cytoskeletal components are damaged by acrolein [5–9 nm microfilament (actin), 8–12 nm intermediate filament (vimentin), and 25 nm microtubule (α- and β-tubulins)].

We have previously reported that acrolein caused apoptosis through conjugation with glyceraldehyde 3-phosphate dehydrogenase (GAPDH), which is translocated to the nucleus (Nakamura et al., 2013), and tissue damage through activation of MMP-9 (Uemura et al., 2017a). Compared to these two effects of acrolein, impairment of microtubule function during brain ischemia may not be so severe damage for brain, although communication between neurons could be weakened through acrolein conjugation with tubulins. However, the effects of damage to tubulins may become greater over time after ischemia.

We have reported that acrolein is strongly involved in the severity of stroke (Tomitori et al., 2005), dementia (Waragai et al., 2012), renal failure (Igarashi et al., 2006), and Sjögren syndrome (Higashi et al.,

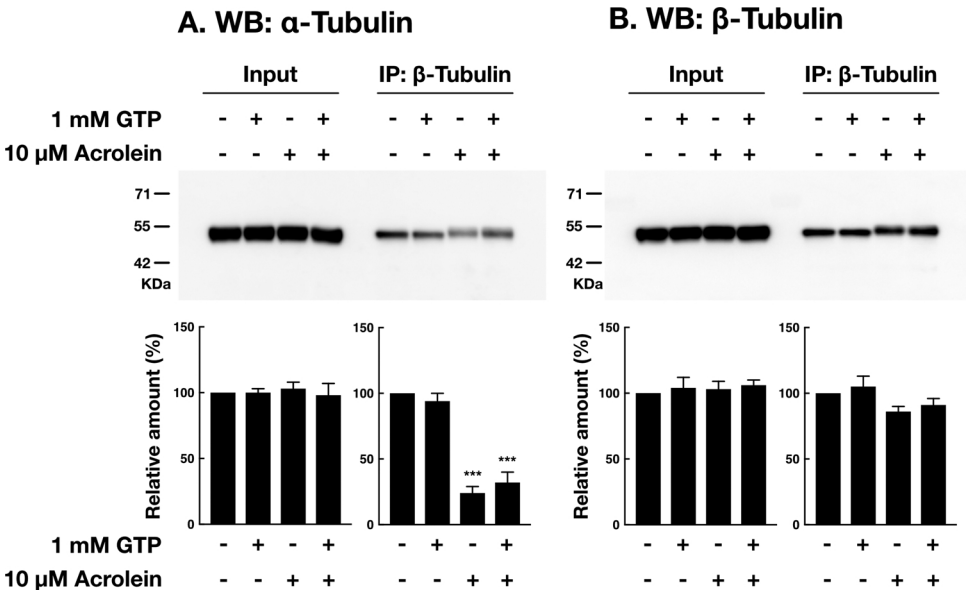

Fig. 6. Effect of acrolein and GTP on the complex formation of α- and β-tubulins. A hundred ng of purified tubulin proteins were incubated with 10 μM of acrolein at 37 °C for 2 h. The degree of the complex formation of α- and β-tubulins in the presence and absence of 1 mM GTP and 10 μM acrolein was measured by immunoprecipitation by antibody against β-tubulin followed by Western blotting with anti-α-tubulin (A) and with anti-β-tubulin (B). Relative amounts were measured from three independent experiments and shown in bar graphs. ***, $p < 0.001$.

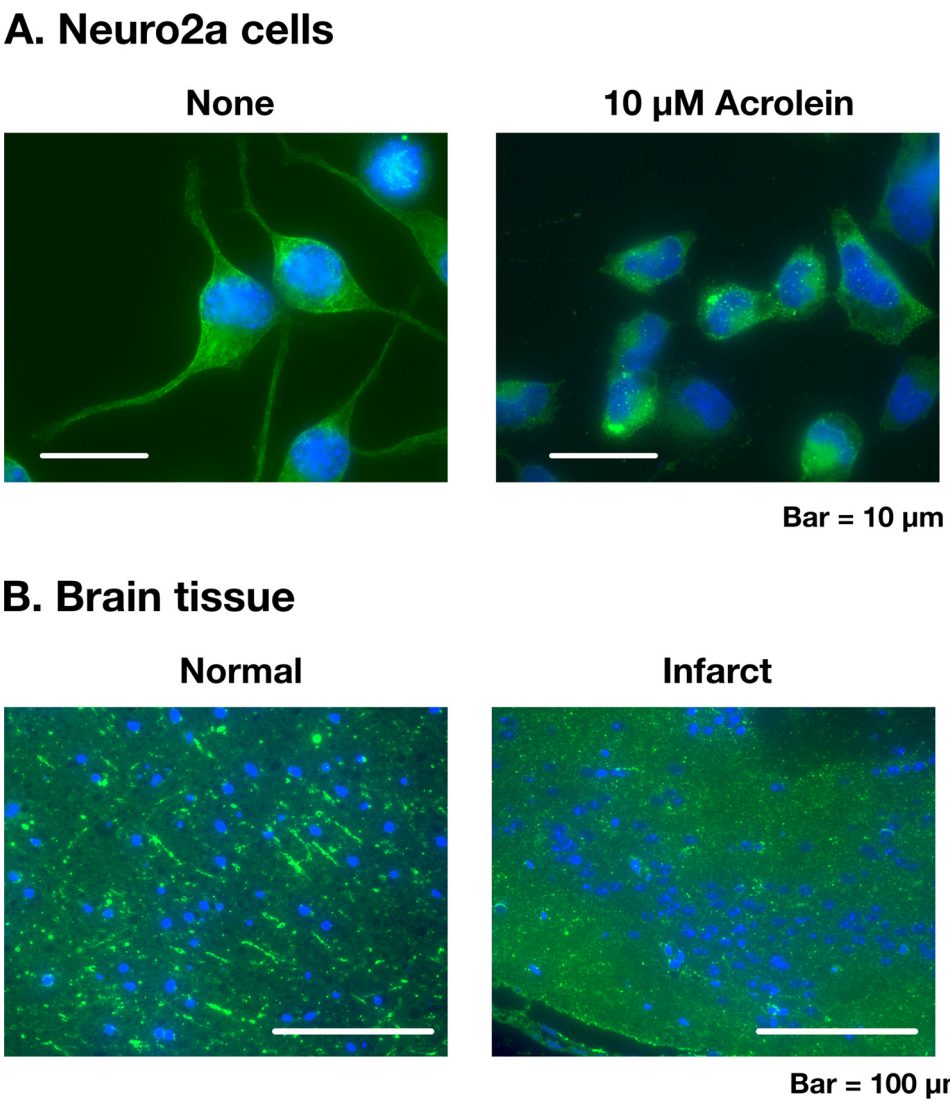

Fig. 7. Microtubule structures in acrolein treated Neuro2a cells and infarct brain. (A) Neuro2a cells were cultured with 10 μM acrolein for 24 h and microtubules were stained using anti-β-tubulin antibody. Bar = 10 μm. (B) A mouse brain was taken out at 24 h after induction of ischemia and microtubules were stained using anti-β-tubulin antibody. Bar = 100 μm. Green and blue fluorescence indicate β-tubulin and nuclei, respectively.

2010). Acrolein is probably involved in other diseases involving cell damage. Indeed, it has been reported that acrolein is involved in neurodegenerative diseases, such as Parkinson's disease (Shamoto-Nagai et al., 2007). and spinal cord injury (Park et al., 2014). The production of acrolein in brain tissue was increased in aged mice due to an increase in spermine oxidase activity (Uemura et al., 2016). This suggests that an increase in acrolein production with age could increase the severity of disorders such as stroke and dementia. Thus, the development of clinically well-tolerated acrolein scavengers such as *N*-acetylcysteine derivatives (Uemura et al., 2018) probably contributes to maintain the quality of life (QOL) of the elderly population.

Conflict of interest

The authors declare that they have no conflicts of interest.

This study was supported by a grant from Chiba Community Service Center and a grant from Supporting Industry Program of NEDO, Japan.

Acknowlegments

We thank Drs. AJ Michael and K. Williams for their help in preparing this manuscript.

References

Alushin, G.M., Lander, G.C., Kellogg, E.H., Zhang, R., Baker, D., Nogales, E., 2014. High-resolution microtubule structures reveal the structural transitions in αβ-tubulin upon GTP hydrolysis. Cell 157, 1117–1129.
Bradley, M.A., Markesbery, W.R., Lovell, M.A., 2010. Increased levels of 4-hydroxynonenal and acrolein in the brain in preclinical Alzheimer disease. Free Radic. Biol. Med. 48, 1570–1576.
Dalle-Donne, I., Carini, M., Vistoli, G., Gamberoni, L., Giustarini, D., Colombo, R., et al., 2007. Actin Cys374 as a nucleophilic target of alpha,beta-unsaturated aldehydes. Free Radic. Biol. Med. 42, 583–598.
Giorgio, M., Trinei, M., Migliaccio, E., Pelicci, P.G., 2007. Hydrogen peroxide: a metabolic by-product or a common mediator of ageing signals? Nat. Rev. Mol. Cell Biol. 8, 722–728.
Higashi, K., Yoshida, M., Igarashi, A., Ito, K., Wada, Y., Murakami, S., et al., 2010. Intense correlation between protein-conjugated acrolein and primary Sjögren's syndrome. Clin. Chim. Acta 411, 359–363.
Igarashi, K., Kashiwagi, K., 2019. The functional role of polyamines in eukaryotic cells. Int. J. Biochem. Cell Biol. 107, 104–115.
Igarashi, K., Ueda, S., Yoshida, K., Kashiwagi, K., 2006. Polyamines in renal failure. Amino Acids 31, 477–483.
Igarashi, K., Uemura, T., Kashiwagi, K., 2018. Acrolein toxicity at advanced age: present and future. Amino Acids 50, 217–228.
Janke, C., Bulinski, J.C., 2011. Post-translational regulation of the microtubule cytoskeleton: mechanisms and functions. Nat. Rev. Mol. Cell Biol. 12, 773–786.
Keates, R.A., 1980. Effects of glycerol on microtubule polymerization kinetics. Biochem. Biophys. Res. Commun. 97, 1163–1169.
Kimes, B.W., Morris, D.R., 1971. Preparation and stability of oxidized polyamines.

Biochim. Biophys. Acta 228, 223–234.
Nakamura, M., Tomitori, H., Suzuki, T., Sakamoto, A., Terui, Y., Saiki, R., et al., 2013. Inactivation of GAPDH as one mechanism of acrolein toxicity. Biochem. Biophys. Res. Commun. 430, 1265–1271.
Park, J., Muratori, B., Shi, R., 2014. Acrolein as a novel therapeutic target for motor and sensory deficits in spinal cord injury. Neural Regen. Res. 9, 677–683.
Pchitskaya, E.I., Zhemkov, V.A., Bezprozvanny, I.B., 2018. Dynamic microtubules in Alzheimer's disease: association with dendritic spine pathology. Biochemistry Mosc. 83, 1068–1074.
Pegg, A.E., 2009. Mammalian polyamine metabolism and function. IUBMB Life 61, 880–894.
Saiki, R., Hayashi, D., Ikuo, Y., Nishimura, K., Ishii, I., Kobayashi, K., et al., 2013. Acrolein stimulates the synthesis of IL-6 and C-reactive protein (CRP) in thrombosis model mice and cultured cells. J. Neurochem. 127, 652–659.
Saiki, R., Nishimura, K., Ishii, I., Omura, T., Okuyama, S., Kashiwagi, K., et al., 2009. Intense correlation between brain infarction and protein-conjugated acrolein. Stroke 40, 3356–3361.
Saiki, R., Park, H., Ishii, I., Yoshida, M., Nishimura, K., Toida, T., et al., 2011. Brain infarction correlates more closely with acrolein than with reactive oxygen species. Biochem. Biophys. Res. Commun. 404, 1044–1049.
Shamoto-Nagai, M., Maruyama, W., Hashizume, Y., Yoshida, M., Osawa, T., Riederer, P., et al., 2007. In parkinsonian substantia nigra, α-synuclein is modified by acrolein, a lipid-peroxidation product, and accumulates in the dopamine neurons with inhibition of proteasome activity. J. Neural Transm. Vienna (Vienna) 114, 1559–1567.
Sharmin, S., Sakata, K., Kashiwagi, K., Ueda, S., Iwasaki, S., Shirahata, A., et al., 2001. Polyamine cytotoxicity in the presence of bovine serum amine oxidase. Biochem. Biophys. Res. Commun. 282, 228–235.
Smith, P.K., Krohn, R.I., Hermanson, G.T., Mallia, A.K., Gartner, F.H., Provenzano, M.D., et al., 1985. Measurement of protein using bicinchoninic acid. Anal. Biochem. 150, 76–85.
Tomitori, H., Usui, T., Saeki, N., Ueda, S., Kase, H., Nishimura, K., et al., 2005. Polyamine oxidase and acrolein as novel biochemical markers for diagnosis of cerebral stroke. Stroke 36, 2609–2613.
Uchida, K., Kanematsu, M., Morimitsu, Y., Osawa, T., Noguchi, N., Niki, E., 1998a. Acrolein is a product of lipid peroxidation reaction. Formation of free acrolein and its conjugate with lysine residues in oxidized low density lipoproteins. J. Biol. Chem. 273, 16058–16066.
Uchida, K., Kanematsu, M., Sakai, K., Matsuda, T., Hattori, N., Mizuno, Y., et al., 1998b. Protein-bound acrolein: potential markers for oxidative stress. Proc. Natl. Acad. Sci. U. S. A. 95, 4882–4887.
Uemura, T., Suzuki, T., Saiki, R., Dohmae, N., Ito, S., Takahashi, H., et al., 2017a. Activation of MMP-9 activity by acrolein in saliva from patients with primary Sjogren's syndrome and its mechanism. Int. J. Biochem. Cell Biol. 88, 84–91.
Uemura, T., Takasaka, T., Igarashi, K., Ikegaya, H., 2017b. Spermine oxidase promotes bile canalicular lumen formation through acrolein production. Sci. Rep. 7, 14841.
Uemura, T., Watanabe, K., Ishibashi, M., Saiki, R., Kuni, K., Nishimura, K., et al., 2016. Aggravation of brain infarction through an increase in acrolein production and a decrease in glutathione with aging. Biochem. Biophys. Res. Commun. 473, 630–635.
Uemura, T., Watanabe, K., Ko, K., Higashi, K., Kogure, N., Kitajima, M., et al., 2018. Protective effects of brain infarction by *N*-acetylcysteine derivatives. Stroke 49, 1727–1733.
Uemura, T., Yerushalmi, H.F., Tsaprailis, G., Stringer, D.E., Pastorian, K.E., Hawel 3rd, L., et al., 2008. Identification and characterization of a diamine exporter in colon epithelial cells. J. Biol. Chem. 283, 26428–26435.
Wang, Y., Casero Jr., R.A., 2006. Mammalian polyamine catabolism: a therapeutic target, a pathological problem, or both? J. Biochem. 139, 17–25.
Waragai, M., Yoshida, M., Mizoi, M., Saiki, R., Kashiwagi, K., Takagi, K., et al., 2012. Increased protein-conjugated acrolein and amyloid-$\beta_{40/42}$ ratio in plasma of patients with mild cognitive impairment and Alzheimer's disease. J. Alzheimers Dis. 32, 33–41.
Yoshida, M., Higashi, K., Kobayashi, E., Saeki, N., Wakui, K., Kusaka, T., et al., 2010. Correlation between images of silent brain infarction, carotid atherosclerosis and white matter hyperintensity, and plasma levels of acrolein, IL-6 and CRP. Atherosclerosis 211, 475–479.
Yoshida, M., Tomitori, H., Machi, Y., Hagihara, M., Higashi, K., Goda, H., et al., 2009. Acrolein toxicity: comparison with reactive oxygen species. Biochem. Biophys. Res. Commun. 378, 313–318.